Luminescence of selective area growth of epitaxial ZnO nanowires and random-growth-oriented nanobelts

2006 Nanotechnology 17 1404

(http://iopscience.iop.org/0957-4484/17/5/040)

INSTITUTE OF PHYSICS PUBLISHING NANOTECHNOLOGY
Nanotechnology **17** (2006) 1404–1407 doi:10.1088/0957-4484/17/5/040

Luminescence of selective area growth of epitaxial ZnO nanowires and random-growth-oriented nanobelts

Hsu-Cheng Hsu[1], Hsin-Ming Cheng[1,2], Chun-Yi Wu[1], Hung-Shang Huang[2], Yi-Chin Lee[1] and Wen-Feng Hsieh[1,3]

[1] Department of Photonics and Institute of Electro-Optical Engineering, National Chiao Tung University, Hsinchu 300, Taiwan
[2] Material and Chemical Research Laboratories, Industrial Technology Research Institute (ITRI), Hsinchu 310, Taiwan

E-mail: wfhsieh@mail.nctu.edu.tw

Received 9 October 2005, in final form 23 December 2005
Published 10 February 2006
Online at stacks.iop.org/Nano/17/1404

Abstract
Epitaxial ZnO nanowires and random-growth-oriented nanobelts were grown on *c*-plane sapphire with and without a pre-coated ZnO epilayer film. On the pre-coated ZnO epilayer, ZnO nanowires are vertically aligned with good in-plane alignment as a result of homoepitaxy, whereas on the bare *c*-plane sapphire, besides a few nanowires vertically aligned with $[0001]_{ZnO} \parallel [0001]_{Al_2O_3}$, the nanowires were properly aligned with three-fold rotation symmetry. The ZnO nanowires are well-defined hexagonal crystals with diameters of 70–500 nm and lengths of up to several micrometres. In the junction regions between the pre-coated epilayer and the bare sapphire surface, however, ZnO nanobelts (nanoribbons) were found. Cathodoluminescence measurements revealed that the emission at 3.26 eV is correlated with free-exciton recombination and the broad green emission at 2.48 eV is attributed to surface defects. The stronger green emission implies that more surface defects exist on the side walls of nanowires and nanobelts. In Raman scattering, the E1(LO) mode is sensitive to the orientation of nanostructure that is consistent with the cathodoluminescence results.

1. Introduction

One-dimensional (1D) ZnO nanostructures such as rods, wires, tubes and belts (ribbons) have attracted increasing attention in recent years because of their superior physical properties [1, 2]. In particular, aligned ZnO nanowires are regarded as promising candidates for nanodevice assembly and in applications for blue–UV light emitters [3–5], field emission devices [6–8] and dye-sensitized solar cells [9]. In fact, the influence of the orientation of ZnO nanowires on optical properties must be understood as it limits the device performance for applications. Therefore, control of the growth direction and shape of the 1D nanostructures and investigation of the correlation between the growth direction and optical properties are significant challenges for device integration. To date, most of the work on ZnO nanostructures has focused on the methods of synthesis and there have been few studies on the influence of their orientation and shape on the optical properties which could limit device performance.

We report on epitaxial ZnO nanowires and nanobelts (nanoribbons) grown on the sapphire *c*-plane with and without a pre-coated ZnO epitaxial film. ZnO nanowires are vertically aligned with good in-plane alignment on the ZnO epilayer; while they are properly aligned with three-fold rotation symmetry on bare sapphire. ZnO nanobelts (nanoribbons) were found at the junction between the epilayer and bare sapphire. The mechanisms of growth and the influence of the orientation and shape of nanowires and nanobelts on the optical properties were studied using structure, cathodoluminescence (CL) and Raman analyses.

[3] Author to whom any correspondence should be addressed.

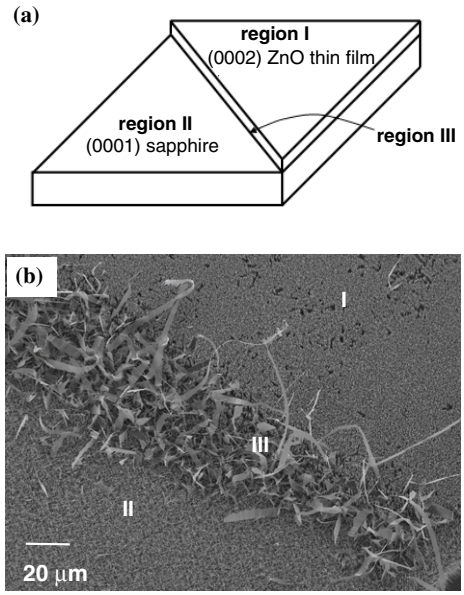

Figure 1. (a) Schematic diagram showing that the substrates can be classified into three regions: region I (ZnO thin film), region II (sapphire) and region III (the junction between the ZnO thin film and the sapphire). (b) Low-magnification SEM images of the synthesized ZnO nanostructure.

2. Experiments

The ZnO nanostructures were fabricated by simple vapour transport deposition [10]. A *c*-plane sapphire buffered with an ZnO epilayer was used as the substrate. The ZnO thin film was grown by pulsed laser deposition using a KrF excimer laser (wavelength 248 nm and pulse duration 25 ns) to ablate a ceramic ZnO target (99.999%) at 600 °C for 2 h and *in situ* annealed for 1 h at 700 °C under a pressure of 10^{-8} Torr. Simultaneously, a metal grid mask covering part of the substrate was used to pattern the ZnO film. The thickness of the ZnO film is about 900 nm. Figure 1(a) shows a sketch of the ZnO/sapphire substrate. The areas of the substrates can be classified into three regions: region I (ZnO thin film), region II (sapphire) and region III (the junction between the ZnO thin film and the sapphire). For x-ray diffraction measurement, the full width at half maximum (FWHM) of the (0002) ω-rocking curve of the thin film is 207 arcsec, indicating a high crystallinity of the thin film. Then the ZnO/sapphire substrate was loaded 2 cm above an alumina boat containing 1 g of zinc metal balls. The boat was put in the middle of a tube furnace. The furnace temperature was increased to 550 °C and high-purity argon gas was then introduced at a flow rate of 500 sccm (standard cubic centimetres per minute). When the growth process was complete, the tube furnace was cooled to room temperature in an Ar gas atmosphere and a white-violet coloured product was found over the substrate.

The morphology and crystal structure of the products were characterized by field emission scanning electron microscopy (FESEM, JEOL 6500), and x-ray diffraction (XRD). CL studies were carried out in the same SEM system and a fully integrated GATAN MonoCL system equipped with a scanning monochromator. The sample was irradiated by an electron beam and the CL emission was collected from the normal to the sample surface. Micro-Raman spectra were measured in the backscattering geometry by a Jobin-Yvon T64000 spectrometer with an Olympus BX40 microscope attachment and equipped with a liquid nitrogen-cooled CCD. The 515 nm line of a frequency-doubled Yb:YAG laser was used as the excitation source. All measurements were performed at room temperature.

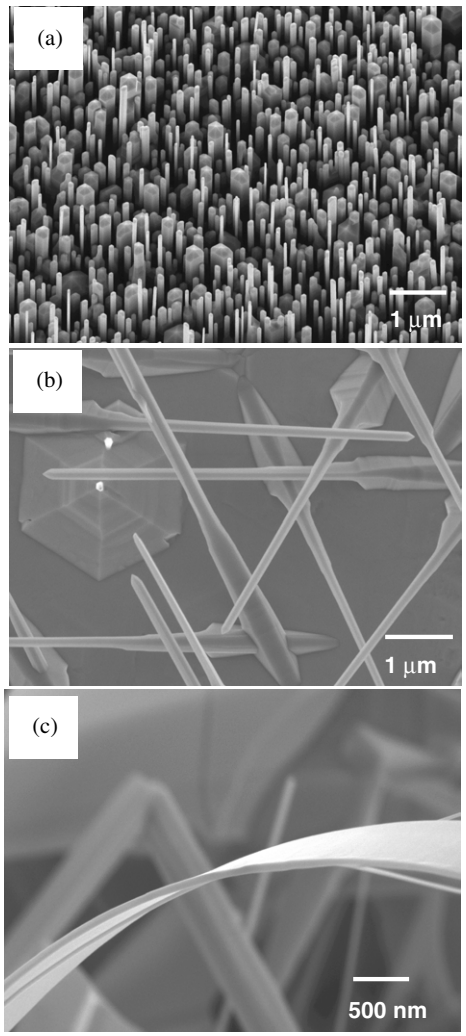

Figure 2. High-magnification SEM images of the synthesized ZnO nanostructure in region I (a), region II (b) and region III (c).

3. Results and discussion

The low-magnification SEM images of the ZnO nanostructure in figure 1(b) show a dense nanostructure grown over the substrate. Figure 2(a) shows a high-magnification image with a 15° inclination of region I. Vertically aligned nanowires have diameters ranging from 80 to 350 nm with well-faceted hexagonal cross sections. A top-view image of the nanowires grown on region II is shown in figure 2(b). There are three clearly noticeable orientations with in-plane components parallel to the sides of an equilateral triangle. Besides some wires oriented perpendicular to the surface that appear as just small bright spots from the top view, a hillock was noted at the

base of these nanowires. The feature of hexagonal hillocks is a typical phenomenon in the epitaxial growth of nanowires [11]. The hillocks form at an early stage to serve as nucleation sites for the subsequent growth of vertical nanowires.

It should be noted that the crystal surface of the pyramidal ZnO island has its unit cell rotated by 30° with respect to that of sapphire to reduce the lattice mismatch between ZnO and sapphire from 32% to 18%. That is similar to the growth of the ZnO epilayer on a *c*-plane sapphire substrate [12]. Baxter *et al* have analysed that the epitaxial relation of nanowires on *c*-plane sapphire [13] should be ZnO$(10\bar{1}0)$ ∥ sapphire$(11\bar{2}0)$ and found that nanowires that were grown at an angle of 51.8° with ZnO[0001] ∥ sapphire $[10\bar{1}4]$ possess excellent lattice symmetry with a lattice match within 2.3%. Combined with the three-fold rotational symmetry of the *c*-plane sapphire, these epitaxial relationships lead to ZnO nanowires being grown on *c*-plane sapphire in one of three directions separated by 120° in projection. In addition, the nanobelts (nanoribbons) were grown in region III, as shown in figure 2(c). The thickness, width and length of the belts are in the ranges of 50–100 nm, 3–6 μm and 5–40 μm, respectively. The nanobelts are unlike the nanowires, whose growth and alignment were strongly related to the ZnO buffer layer and bare *c*-plane sapphire.

The growth mechanism of ZnO nanowires in region I is probably governed by a vapour–solid process [14]. Under zinc-rich ambient conditions a thin film will prefer column growth [15] and the growth rate of the (0001) plane is greater than that of the others. Since no extra O_2 was added in our processing furnace, anisotropic growth should take place. The melting points of Zn and ZnO_x $(x < 1)$ are approximately 419 °C, and liquid Zn should form and react with residual oxygen to form ZnO_x in the initial period of nucleation [16]. Simultaneously, the liquid phase Zn or ZnO_x also serves as the eutectic solvent for the oxide species. The anisotropic growth of the crystal causes formation of a ZnO nanostructure with a high aspect ratio and the ZnO nanowires are preferentially oriented along the *c*-axis direction due to the growth rate being fastest in this direction. Such a 'self-catalytic' mechanism has been used to explain the formation of 1D metal oxide nanostructures [16–18].

Nevertheless, the formation of nanobelts is another issue. We believe that this is related to the crystal plane on the step wall of the ZnO film or somehow related to the gas turbulence at the step of the film. Supersaturation of Zn vapour occurs at the step, leading to an enlargement of the crystal dimensions.

CL spectroscopy was carried out for all nanostructures. Figures 3(a)–(c) show the CL spectra of vertically aligned nanowires, tilted-growth nanowires and nanobelts, respectively. All the emission bands are composed of a sharp UV band around 3.26 eV and a green band around 2.48 eV. The UV peak is correlated with the free exciton emission, whereas the broad green band is commonly observed in the photoluminescence (PL) spectra of nominally undoped ZnO thin films [19, 20] and nanostructures [21–23] Recent studies on the recombination mechanisms responsible for the green emission in ZnO phosphors have suggested that the green PL arises from the recombination of electrons in singly occupied oxygen vacancies with photogenerated holes in the valence band [24]. The vacancy defect centres exist primarily in the thin (∼30 nm) electron-depletion layer near the surface of the ZnO [24].

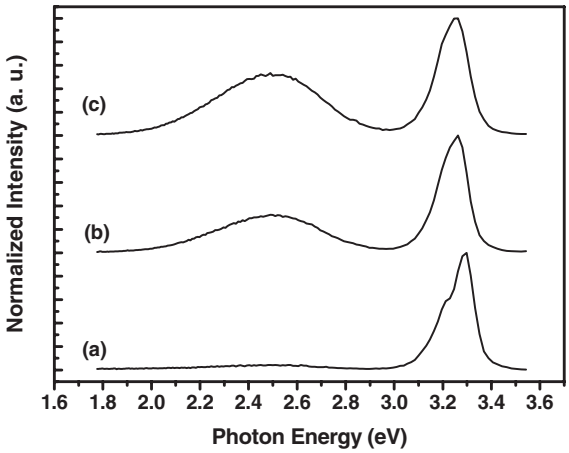

Figure 3. Room-temperature PL spectra from (a) the vertically aligned ZnO nanowires grown in region I, (b) tilt-aligned ZnO nanowires in region II and (c) random-growth-oriented nanobelts in region III.

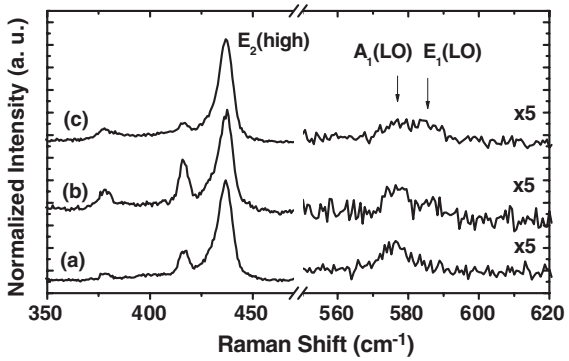

Figure 4. Raman spectra obtained from (a) the vertically aligned ZnO nanowires grown in region I, (b) the tilt-aligned ZnO nanowires in region II and (c) random-growth-oriented nanobelts in region III.

The vertically aligned nanowires have the highest intensity ratio of UV to green emission, whereas the nanobelts have the lowest ratio. A previous study on vertically aligned ZnO nanowires found that the intensity of the UV/green emission has a maximum (minimum) along (perpendicular to) the *c*-axis of the ZnO nanowire, and it was proposed that the green emission is generated and emitted from the side walls of the nanowires [25]. Shalish *et al* [26] show that the intensity ratio of UV to green emission decreases when the diameter of the ZnO nanowires is reduced. They proposed a *surface recombination layer approximation* to confirm that surface recombination dominates the luminescence spectra with diminishing diameter. In our experiment, the emission was collected from normal to the sample surface; there was more UV emission along the *c*-axis from vertically aligned nanowires than from tripod wires and nanobelts. This may be the reason why it is easier to observe the green emission from the randomly oriented nanowires [14, 27] and nanobelts [28, 29].

Figure 4 shows typical micro-Raman spectra of ZnO nanostructures. The wurtzite structure of ZnO belongs to the space group C_{6v}^4 $(P6_3mc)$ with two formula units in a primitive

cell [30]. The group theory predicts the existence of the following optic modes: $A_1 + 2B_1 + E_1 + 2E_2$ at the Γ point of the Brillouin zone; B_1 (low) and B_1 (high) modes are normally silent; A_1, E_1, and E_2 modes are Raman active; and A_1 and E_1 are also infrared active. Due to overlapping of several Raman modes of ZnO materials with the sapphire substrate [30–33], one has to analyse the spectra very carefully, for example the E_1(TO) mode of ZnO overlaps with the E_g mode of sapphire at 378 cm^{-1} and the A_1(LO) mode of ZnO overlaps with another E_g mode of sapphire near 578 cm^{-1}. In addition, the spectral peak at 417 cm^{-1} is the distinct sapphire A_{1g} mode. In spite of these features in Raman spectra, we still observe a E_2 (high) mode at 437 cm^{-1} with a width of 10 cm^{-1}, indicating good crystal quality. Because the propagation direction of E_1(LO) parallel to $[0\bar{1}1]$ is parallel neither to the XY-plane nor to the Z-axis [33] in the backscattering configuration, the E_1(LO) mode near 586 cm^{-1} cannot be observed from the vertically aligned nanowires but can be observed from the tilted nanowires and randomly oriented nanobelts. This Raman mode for the tilted nanowires and randomly oriented nanobelts is more efficiently collected than for the vertical nanowires. The Raman spectra of these ZnO nanostructures strongly depend on the collecting configuration and the crystal face and are consistent with the CL results.

4. Conclusion

In summary, we found that ZnO nanowires grown on a pre-coated ZnO epilayer are vertically aligned with good in-plane alignment as a result of homoepitaxy from CL and Raman analyses. However, besides a few nanowires that were vertically aligned with $[0001]_{ZnO} \parallel [0001]_{\alpha\text{-}Al_2O_3}$ on the bare c-plane sapphire, the nanowires were properly aligned with three-fold rotation symmetry. Furthermore, ZnO nanobelts were found at the junctions between the epilayer and the bare sapphire. The emission at 3.26 eV is correlated with the recombination of free exciton and a broad green emission at 2.48 eV is attributed to surface defects at room temperature. The vertically aligned nanowires have the highest ratio of UV emission to green emission, whereas the nanobelts have the lowest ratio. This implies that there are more surface defects existing on the side wall of the nanowires and nanobelts due to recombination between holes trapped at the surface defects or electrons trapped at the oxygen vacancy. We demonstrated that not only the photoemission but also the phonon properties are dependent on the configuration and crystal facet of the nanostructures.

Acknowledgments

This work was partially supported by the National Science Council (NSC) of the Republic of China under grant 94-2112-M009-015. HCH gratefully thanks NSC for providing a fellowship. We also thank the NanoTechnology Research Centre (NTRC) at ITRI for facility support.

References

[1] Wang Z L 2004 *J. Phys.: Condens. Matter* **16** R829
[2] Heo Y W, Norton D P, Tien L C, Kwon Y, Kang B S, Ren F, Pearton S J and LaRoche J R 2004 *Mater. Sci. Eng.* R **47** 1
[3] Huang M H, Mao S, Feick H, Yan H Q, Wu Y Y, Kind H, Weber E, Russo R and Yang P D 2001 *Science* **292** 1897
[4] Park W I and Yi G C 2004 *Adv. Mater.* **16** 87
[5] Konenkamp R, Word R C and Schlegel C 2004 *Appl. Phys. Lett.* **85** 6004
[6] Lee C J, Lee T J, Lyu S C, Zhang Y, Ruh H and Lee H J 2002 *Appl. Phys. Lett.* **81** 3648
[7] Tseng Y K, Huang C J, Cheng H M, Lin I N, Liu K S and Chen I C 2003 *Adv. Funct. Mater.* **13** 811
[8] Li S Y, Lin P, Lee C Y and Tseng T Y 2004 *J. Appl. Phys.* **95** 3711
[9] Baxter J B and Aydil E S 2005 *Appl. Phys. Lett.* **86** 053114
[10] Cheng H M, Hsu H C, Yang S, Wu C Y, Lee Y C, Lin L J and Hsieh W F 2005 *Nanotechnology* **16** 2882
[11] Fan H J, Bertram F, Dadgar A, Christen J, Krost A and Zacharias M 2004 *Nanotechnology* **15** 1401
[12] Chen Y F, Bagnall D M, Koh H J, Park K T, Hiraga K, Zhu Z Q and Yao T 1998 *J. Appl. Phys.* **84** 3912
[13] Baxter J B and Aydil E S 2005 *J. Cryst. Growth* **274** 407
[14] Hsu H C, Tseng Y K, Cheng H M, Kuo J H and Hsieh W F 2004 *J. Cryst. Growth* **261** 520
[15] Chen Y F, Ko H J, Hong S K, Yao T and Segawa Y 2002 *Appl. Phys. Lett.* **80** 1358
[16] Yao B D, Chan Y F and Wang N 2002 *Appl. Phys. Lett.* **81** 457
[17] Fan H J, Scholz R, Kolb F M and Zacharias M 2005 *Appl. Phys. Lett.* **85** 4142
[18] Dang H Y, Wang J and Fan S S 2003 *Nanotechnology* **14** 738
[19] Bethke S, Pan H and Wesseis B W 1988 *Appl. Phys. Lett.* **52** 136
[20] Muth J F, Kolbas R M, Sharma A K, Oktyabrsky S and Narayan J 1999 *J. Appl. Phys.* **85** 7884
[21] Huang M H, Wu Y, Feick H, Tran N, Weber E and Yang P D 2001 *Adv. Mater.* **13** 113
[22] Banerjee D, Lao J Y, Wang Z D, Huang J Y, Ren Z F, Steeves D, Kimball B and Sennett M 2003 *Appl. Phys. Lett.* **83** 2061
[23] Roy V A L, Djurisic A B, Chan W K, Gao J, Lui H F and Surya C 2003 *Appl. Phys Lett.* **83** 141
[24] Vanheusden K, Warren W L, Seager C H, Tallant D R, Voigt J A and Gnade B E 1996 *J. Appl. Phys.* **79** 7983
[25] Hsu N E, Hung W K and Chen Y F 2004 *J. Appl. Phys.* **96** 4671
[26] Shalish I, Temkin H and Narayanamurti V 2004 *Phys. Rev.* B **69** 245401
[27] Hu J Q, Li Q, Wong N B, Lee C S and Lee S T 2002 *Chem. Mater.* **14** 1216
[28] Li Y B, Bando Y, Sato T and Kurashima K 2002 *Appl Phys. Lett.* **81** 144
[29] Wei Q, Meng G W, An X H, Hao Y F and Zhang L D 2005 *Nanotechnology* **16** 2561
[30] Calleja J M and Cardona M 1977 *Phys. Rev.* B **16** 3753
[31] Decremps F, Pellicer-Porres J, Saitta A M, Chervin J C and Polian A 2002 *Phys. Rev.* B **65** 092101
[32] Ashkenov N *et al* 2003 *J. Appl. Phys.* **93** 126
[33] Arguello C A, Rousseau D L and Porto S P S 1969 *Phys. Rev.* **181** 1351